

# Neutrino reactions via neutral and charged current by Quasi-particle Random Phase Approximation(QRPA)

Myung-Ki Cheoun<sup>1)\*</sup>, Eunja Ha<sup>1)</sup>, K. S. Kim<sup>2)†</sup>, Toshitaka Kajino<sup>3,4)</sup>

1) *Department of Physics, Soongsil University, Seoul 156-743, Korea*

2) *School of Liberal Arts and Science,*

*Korea Aerospace University, Koyang 412-791, Korea*

3) *National Astronomical Observatory, Mitaka, Tokyo 181-8589, Japan*

4) *Department of Astronomy, Graduate School of Science,  
University of Tokyo, 7-3-1 Hongo, Tokyo 113-0033, Japan*

We developed the quasi-particle random phase approximation (QRPA) for the neutrino scattering off even-even nuclei via neutral current (NC) and charged current (CC). The QRPA has been successfully applied for the  $\beta$  and  $\beta\beta$  decay of relevant nuclei. To describe neutrino scattering, general multipole transitions by weak interactions with a finite momentum transfer are calculated for NC and CC reaction with detailed formalism. Since we consider neutron-proton (np) pairing as well as neutron-neutron (nn) and proton-proton (pp) pairing correlations, the nn + pp QRPA and np QRPA are combined in a framework, which enables to describe both NC and CC reactions in a consistent way. Numerical results for  $\nu$ - $^{12}\text{C}$ ,  $^{-56}\text{Fe}$  and  $^{-56}\text{Ni}$  reactions are shown to comply with other theoretical calculations and reproduce well available experimental data.

PACS numbers: 21.60.Jz, 23.40.Hc

## I. INTRODUCTION

Neutrino ( $\nu$ ) (antineutrino ( $\bar{\nu}$ )) scattering with a complex nucleus plays important roles on understanding the nuclear structure probed by weak interaction [1–3] as well as relevant  $\nu$  parameters in the  $\nu$  physics [4, 5], such as mass hierarchy and mixing angle  $\theta_{13}$  through

---

\* Corresponding author : cheoun@ssu.ac.kr

† kyungsik@hau.ac.kr

detailed analysis of nuclear abundances in the core collapsing supernova (SN) explosion. Recently, lots of interests have been focused on the  $\nu$  process [4–7] in the nucleosynthesis because the emitted neutrino flux is expected to be large enough to excite the relevant nuclei in spite of the small cross section due to the weak interaction. Therefore cross sections for the neutrino(antineutrino)-nucleus ( $\nu(\bar{\nu}) - A$ ) scattering with relevant nuclei are to be treated as important input data for a network calculation estimating the nuclear abundances, in specific, for the weak rapid process [8].

Incident  $\nu(\bar{\nu})$  energies exploited in the SN explosion [4, 5] are focused on the energy range from a few to tens of MeV because relevant  $\nu(\bar{\nu})$  energy spectra emitted from a proto-neutron star are presumed to be peaked mostly around the energy region by following a Fermi-Dirac distribution given by temperature ( $T$ ) and chemical potential ( $\alpha$ ) [9].

$$f(E_\nu) = \frac{1}{F(\alpha)T^3} \frac{E_\nu^2}{\exp[(E_\nu/T) - \alpha] - 1} , \quad (1)$$

where  $F(\alpha)$  is a normalization factor. ( $T, \alpha$ ) can be chosen for neutrino types. Therefore, the  $\nu(\bar{\nu}) - A$  reactions are usually sensitive on the collective motions of nucleons inside nuclei and proceed via two-step processes, *i.e.* the target nuclei are excited by the incident  $\nu(\bar{\nu})$  and decayed to the lower energy states with the emission of some particles [9].

The excitation occurs through various transitions, *i.e.* super allowed Fermi ( $J^\pi = 0^+$ ), allowed Gamow Teller (GT) ( $J^\pi = 1^+$ ), spin dipole ( $J^\pi = 0^-, 1^-, 2^-$ ), and other higher multipole transitions. Therefore dominant contributions of the two-step process stem from discrete and giant resonance (GR) states of the compound nucleus. Their typical excitation energy is below tens of MeV. It should be noticed that not only isobaric analogue state (IAS) and GT transitions but also contributions from higher order multipoles could play important roles in the  $\nu - A$  reaction [3, 10].

In the experimental side, only a few data measured from accelerated-based  $\nu$  facilities, which are deduced mainly from  $^{12}\text{C}$ , exist exclusively for the first stage of the two step processes, that is, the formation of compound nuclei. They have been reported as  $\nu$  flux averaged total cross sections in the last decade [11–15]

$$\langle \sigma_\nu \rangle = \frac{\int dE_\nu \sigma_\nu(E_\nu) f(E_\nu)}{\int dE_\nu f(E_\nu)} , \quad (2)$$

where  $\sigma_\nu(E_\nu)$  and  $f(E_\nu)$  are  $\nu - A$  cross section and corresponding neutrino flux. Unfortunately, there are no data including the decay processes, that is, the second stage in the

two-step process. Neutrino facilities usually used neutrino source from the pion decay at rest (DAR) and in flight (DIF). For the DAR neutrino, one obtains continuous spectrum for  $\nu_e$ , which is given as the Michel spectrum

$$f(E_\nu) = \frac{96E_\nu^2}{m_\pi^4}(m_\mu - 2E_\nu) , \quad (3)$$

and different continuous spectrum for  $\bar{\nu}_\mu$  [11], and mono-energetic  $\nu_\mu$  fixed as 29.8 MeV. Continuous  $\nu_\mu$  spectrum is obtained from the DIF neutrino. Recently, another new method for the production of intense and pure  $\nu$  beams has been proposed, called the beta-beam [16, 17], which is originally planned to study the CP violation in the lepton sector. The concept of the beta-beam is designed by using boosted radioactive ions which can be decayed with emitting neutrinos. For the study of fundamental interactions and nuclear structure, this new future facility may produce monochromatic  $\nu$  beams through the electron capture of radioactive ion beam. Of course, these beams depend on the existence of ions decaying through the electron capture. It was also suggested how to obtain a mono-energetic  $\nu$  beam by using an electron capture process on a nucleus [18, 19].

Most data are focused on  $^{12}\text{C}$  target because the  $^{12}\text{C}$  nucleus itself serves as a  $\nu(\bar{\nu})$  detector. Data for the inclusive reaction,  $^{12}\text{C}(\nu_e, e^-)^{12}\text{N}^*$ , show about  $3.3 \sim 6.7$  in the  $10^{-42} \text{ cm}^2$  unit including indicated experimental error bars, while data for the exclusive reaction like  $^{12}\text{C}(\nu_e, e^-)^{12}\text{N}_{g.s.}$  and  $^{12}\text{C}(\nu, \nu')^{12}\text{C}$  (15.11 MeV) for the DAR neutrino are restricted to  $6.07 \sim 10.4$  and  $8.5 \sim 12.3$  in the same unit, respectively [11–15].

The  $\nu$  scattering data based on accelerator are mainly restricted to the formation of compound nuclei. But the excited states in compound nuclei subsequently decays into other nuclei with emitting particles such as proton, neutron, alpha,  $\gamma$ , and so on [3, 5]. To describe the decay processes at the second stage, one needs additional calculations for branching ratios into the decay processes like Hauser-Feshbach (HF) statistical model [3, 20]. Any final state interactions (FSI) between outgoing particles and residual nuclei should be also taken into account at this stage. Of course, for the nuclear abundance, both two stages are to be successively considered.

Before presenting our results, we briefly summarize recent theoretical status about  $\nu - A$  scattering with detailed references. Since the pioneering work by J. S. Cornell *et al.*[2], which exactly predicted the  $\nu - ^{12}\text{C}$  reaction via charged current 20 years ago before the advent of the data, many theoretical calculations[2, 3, 10, 21–23, 25] have been done and compared to the experimental data, mainly to the  $\nu - ^{12}\text{C}$  reaction. Conventional

approaches for the  $\nu - A$  scattering in the low energy region are shell model (SM)[3], random phase approximation (RPA)[21], and Quasi-particle RPA (QRPA)[10, 21].

Although results of most SM calculations [3, 21] converge more or less on the experimental data, they inevitably depend on the particle model space, the given Hamiltonian, the so called  $g_A$  quenching, and so on. The RPA [21] and the QRPA [10, 21] calculation usually overestimated the data by a factor of  $4 \sim 5$ . More detailed summaries of the calculations are presented at Ref.[9, 21, 23]. But recent calculation by proton-neutron QRPA [10] shows more improved results by simultaneously considering other relevant processes.

In medium heavy or heavy nuclei, neutron-proton (np) pairing as well as proton-proton (pp) and neutron-neutron (nn) pairing could be important because of the small energy gap due to the neutron excess, although its empirical magnitude is small compared to those of light nuclei [24]. Moreover the np pairing enables us to consistently describe the CC and NC reactions in a framework, as shown later on.

On the other hand, the Continuum RPA (CRPA) [22, 23, 25, 26] includes continuum excitation spectrum in the quasi-elastic (QE) region in addition to the discrete and GR states, while most of SM, RPA and QRPA do not take explicitly the contribution from the QE region into account. The CRPA shows almost identical results compared to other approaches for the  $\nu - A$  scattering by the DAR neutrino, so that the QE contribution seems to be small enough to be neglected on a few tens of MeV region.

In this work, we present our QRPA formalism for the  $\nu - A$  reaction via CC and NC type by including nn, pp and np pairing and compare them with the available experimental data and other calculations. Our QRPA has successfully described  $\beta$ ,  $2\nu\beta\beta$  and  $0\nu2\beta$  decays [24]. Fairly reasonable results with the experimental data are obtained. In Sec.II, we presented our whole formulas for  $\nu - A$  scattering, which is based on the Bardeen Cooper Schriffer (BCS) theory for the ground state description and the QRPA for the transition to the excited state. Relevant weak transitions and their operators are also summarized in Sec.II with the cross section formula. Numerical results and discussions are done in Sec.III. Summary and conclusions are given at Sec.IV.

## II. FORMALISM

### A. Description of ground state with np pairing

We start from the following hamiltonian

$$H = H_0 + H_{int}, \quad H_0 = \sum_{a'\alpha} \epsilon_{a\alpha} c_{a\alpha}^+ c_{a\alpha}, \quad H_{int} = \sum_{a'b'c'd', \alpha\beta\gamma\delta} V_{a\alpha b\beta c\gamma d\delta} c_{a\alpha}^+ c_{b\beta}^+ c_{d\delta} c_{c\gamma}, \quad (4)$$

where the interaction matrix  $V$  is the antisymmetrized interaction with the Baranger hamiltonian [27] in which two  $\frac{-1}{2}$  factors, from J and T coupling, are included, so that the  $H_{int}$  in Eq.(4) is equivalent to the usual  $H_{int} = \frac{1}{4} \sum_{a'b'c'd', \alpha\beta\gamma\delta} \tilde{V}_{a\alpha b\beta c\gamma d\delta} c_{a\alpha}^+ c_{b\beta}^+ c_{d\delta} c_{c\gamma}$ . Roman letters indicate the quantum numbers of the nucleon states, i.e.  $a = (n_a, l_a, j_a)$ . But Roman letters with prime include also the magnetic quantum number i.e.  $a' = (n_a, l_a, j_a, m_a)$ . The isospin of real particles is denoted as a Greek letter while the isospin of quasi-particles is expressed as a Greek letter with prime. The operator  $c_{a\alpha}^+$ ,  $c_{a\alpha}$  stand for the usual creation and destruction operators of the nucleons in the state of  $a'$  with an isospin  $\alpha$ .  $c_{\bar{d}\delta} = c_{n_d, l_d, j_d, -m_d} (-)^{j_d - m_d}$  is the time reversed operator of  $c_{d\delta}$ .

We transform this hamiltonian by the general HFB transformation to quasi-particles,

$$a_{c\mu'}^+ = \sum_{d'\delta} (u_{c'\mu'd'\delta} c_{d\delta}^+ + v_{c'\mu'd'\delta} c_{\bar{d}\delta}), \quad a_{\bar{c}\mu'} = \sum_{d'\delta} (u_{c'\mu'd'\delta}^* c_{\bar{d}\delta} + v_{c'\mu'd'\delta}^* c_{d\delta}^+). \quad (5)$$

Here time reversal and spherical symmetries for the nuclei are presumed, so that we do not mix different single particle angular momentum states in Eq.(5). Then the Hamiltonian can be represented in terms of the quasi-particles as follows

$$H' = H'_0 + \sum_{a'\alpha'} E_{a\alpha'} a_{a\alpha'}^+ a_{a\alpha'} + H_{qp.int}. \quad (6)$$

Using the transformation of Eq.(5) we obtain the following HFB equation

$$\begin{pmatrix} \epsilon_p - \lambda_p & 0 & \Delta_{p\bar{p}} & \Delta_{p\bar{n}} \\ 0 & \epsilon_n - \lambda_n & \Delta_{n\bar{p}} & \Delta_{n\bar{n}} \\ \Delta_{p\bar{p}} & \Delta_{p\bar{n}} & -\epsilon_p + \lambda_p & 0 \\ \Delta_{n\bar{p}} & \Delta_{n\bar{n}} & 0 & -\epsilon_n + \lambda_n \end{pmatrix}_c \begin{pmatrix} u_{\alpha'p} \\ u_{\alpha'n} \\ v_{\alpha'p} \\ v_{\alpha'n} \end{pmatrix}_c = E_{c\alpha'} \begin{pmatrix} u_{\alpha'p} \\ u_{\alpha'n} \\ v_{\alpha'p} \\ v_{\alpha'n} \end{pmatrix}_c \quad (7)$$

, where  $E_{c\alpha'}$  is the energy of a quasi particle with the isospin quantum number  $\alpha'$  in the state  $c$ . If we neglect  $\Delta_{np}$ , this equation reduces to the standard BCS equation. The pairing potentials  $\Delta_p$ ,  $\Delta_n$  and  $\Delta_{pn}$  in Eq.(7) are detailed at Ref [24].

## B. QRPA coupled by neutron-proton pairing

Excited states,  $|m; J^\pi M\rangle$ , in a compound nucleus, are generated from the ground state of the target nucleus, which is an even-even nucleus and acts as the BCS vacua for the quasi-particle, by operating the following one phonon operator to the initial nucleus

$$Q_{JM}^{+,m} = \sum_{k\mu' l\nu'} [X_{(k\mu' l\nu' J)}^m C^+(k\mu' l\nu' JM) - Y_{(k\mu' l\nu' J)}^m \tilde{C}(k\mu' l\nu' JM)] , \quad (8)$$

where

$$C(k\mu' l\nu' JM) = \sum_{m_k m_l} C_{j_k m_k j_l m_l}^{JM} a_{l\nu'} a_{k\mu'} , \quad \tilde{C}(k\mu' l\nu' JM) = (-)^{J-M} C(k\mu' l\nu' J - M) \quad (9)$$

with a quasi-particle annihilation operator  $a_{l\nu'}$  and Clebsh-Gordan coefficient  $C_{j_k m_k j_l m_l}^{JM}$ . If neutron-proton pairing is neglected, the phonon operator decouples to two phonon operators. One is for the charge changing reaction such as beta decay and CC neutrino reaction. The second is for the charge conserving such as electro-magnetic and NC neutrino reactions. The amplitudes  $X_{\alpha\alpha, b\beta}$  and  $Y_{\alpha\alpha, b\beta}$ , which stand for forward and backward going amplitudes from state  $a\alpha$  to  $b\beta$ , are obtained from the following QRPA equation, whose detailed derivation was also shown at Ref. [24]

$$\begin{pmatrix} A_{klab}^{1111} & A_{klab}^{1122} & A_{klab}^{1112} & B_{klab}^{1111} & B_{klab}^{1122} & B_{klab}^{1112} \\ A_{klab}^{2211} & A_{klab}^{2222} & A_{klab}^{2212} & B_{klab}^{2211} & B_{klab}^{2222} & B_{klab}^{2212} \\ A_{klab}^{1211} & A_{klab}^{1222} & A_{klab}^{1212} & B_{klab}^{1211} & B_{klab}^{1222} & B_{klab}^{1212} \\ -B_{klab}^{1111} & -B_{klab}^{1122} & -B_{klab}^{1112} & -A_{klab}^{1111} & -A_{klab}^{1122} & -A_{klab}^{1112} \\ -B_{klab}^{2211} & -B_{klab}^{2222} & -B_{klab}^{2212} & -A_{klab}^{2211} & -A_{klab}^{2222} & -A_{klab}^{2212} \\ -B_{klab}^{1211} & -B_{klab}^{1222} & -B_{klab}^{1212} & -A_{klab}^{1211} & -A_{klab}^{1222} & -A_{klab}^{1212} \end{pmatrix} \begin{pmatrix} \tilde{X}_{(a1b1)J}^m \\ \tilde{X}_{(a2b2)J}^m \\ \tilde{X}_{(a1b2)J}^m \\ \tilde{Y}_{(a1b1)J}^m \\ \tilde{Y}_{(a2b2)J}^m \\ \tilde{Y}_{(a1b2)J}^m \end{pmatrix} = \hbar\Omega^m \begin{pmatrix} \tilde{X}_{(k1l1)J}^m \\ \tilde{X}_{(k2l2)J}^m \\ \tilde{X}_{(k1l2)J}^m \\ \tilde{Y}_{(k1l1)J}^m \\ \tilde{Y}_{(k2l2)J}^m \\ \tilde{Y}_{(k1l2)J}^m \end{pmatrix} . \quad (10)$$

The A and B matrices are given by

$$\begin{aligned} A_{klab}^{\gamma' \delta' \mu' \nu'} &= (E_{k\gamma'} + E_{l\delta'}) \delta_{ka} \delta_{\gamma' \mu'} \delta_{lb} \delta_{\delta' \nu'} \\ &- \sigma_{k\gamma' l\delta'} \sigma_{a\mu' b\nu'} \sum_{\alpha\beta\gamma\delta} [G(k\alpha l\beta a\gamma b\delta J) (u_{k\gamma' \alpha} u_{l\delta' \beta} u_{a\mu' \gamma} u_{b\nu' \delta} + v_{k\gamma' \alpha} v_{l\delta' \beta} v_{a\mu' \gamma} v_{b\nu' \delta}) \\ &+ F(k\alpha l\beta a\gamma b\delta J) (u_{k\gamma' \alpha} v_{l\delta' \beta} u_{a\mu' \gamma} v_{b\nu' \delta} + v_{k\gamma' \alpha} u_{l\delta' \beta} v_{a\mu' \gamma} u_{b\nu' \delta}) \\ &- (-1)^{j_{k'} + j_{l'} + J} F(k\alpha l\beta b\delta a\gamma J) (u_{k\gamma' \alpha} v_{l\delta' \beta} u_{b\nu' \gamma} v_{a\mu' \delta} + v_{k\gamma' \alpha} u_{l\delta' \beta} v_{b\nu' \gamma} u_{a\mu' \delta}) ] , \end{aligned} \quad (11)$$

$$\begin{aligned}
B_{klab}^{\gamma' \delta' \mu' \nu'} &= -\sigma_{k\gamma' l\delta'} \sigma_{a\mu' b\nu'} \sum_{\alpha\beta\gamma\delta} [-G(k\alpha l\beta a\gamma b\delta J)(u_{k\gamma'\alpha} u_{l\delta'\beta} v_{a\mu'\gamma} v_{b\nu'\delta} + v_{k\gamma'\alpha} v_{l\delta'\beta} u_{a\mu'\gamma} u_{b\nu'\delta}) \\
&+ F(k\alpha l\beta a\gamma b\delta J)(u_{k\gamma'\alpha} v_{l\delta'\beta} v_{a\mu'\gamma} u_{b\nu'\delta} + v_{k\gamma'\alpha} u_{l\delta'\beta} u_{a\mu'\gamma} v_{b\nu'\delta}) \\
&- (-1)^{j_{k'}+j_{l'}+J} F(k\alpha l\beta b\delta a\gamma J)(u_{k\gamma'\alpha} v_{l\delta'\beta} u_{a\mu'\gamma} v_{b\nu'\delta} + v_{k\gamma'\alpha} u_{l\delta'\beta} v_{a\mu'\gamma} u_{b\nu'\delta})] ,
\end{aligned}$$

where  $u$  and  $v$  coefficients related to the occupation probabilities of a given state are determined from the HFB calculation in Eq.(7) with the pairing strength  $g_{nn}$ ,  $g_{pp}$  and  $g_{np}$  adjusted to the empirical pairing gaps  $\Delta_{nn}$ ,  $\Delta_{pp}$  and  $\delta_{np}$ , respectively [24].  $E_{k\gamma'}$  indicates the quasi-particle energy of the state  $k$  with the quasi-particle isospin  $\gamma'$ , and  $\sigma_{k\gamma' l\delta'} = 1$  if  $k = l$  and  $\gamma' = \delta'$ , otherwise  $\sigma_{k\gamma' l\delta'} = \sqrt{2}$ . The  $G(F)$  matrices are two body particle - particle (hole) matrix elements obtained as solutions of the following Bethe - Goldstone equation, called as  $\mathcal{G}$  matrix,

$$\mathcal{G}(w)_{ab,cd} = V_{ab,cd}^{OBEP} + V_{ab,cd}^{OBEP} \frac{Q_p}{w - H_0} \mathcal{G}(w)_{ab,cd} , \quad (13)$$

where  $a, b, c, d$  indicate the single nucleon basis states characterized by oscillator type wave functions with single particle energies from the Woods-Saxon potential.  $H_0$  is the harmonic oscillator hamiltonian and  $Q_p$  is the Pauli operator.  $V_{ab,cd}^{OBEP}$  is the phenomenological nucleon-nucleon potential. We used the one boson exchange potential of the Bonn group [28]. Of course, one can use effective interactions for the 2-body interactions, such as the effective Skyrme force and the surface delta interactions [10] instead of the  $\mathcal{G}$ -matrix.

### C. Description of CC and NC reaction

Under the second quantization, matrix elements of any transition operator  $\hat{O}$  between a ground state and an excited state  $|\omega; JM\rangle$  can be factored as follows

$$\langle QRPA || \hat{O}_\lambda || \omega; JM \rangle = [\lambda]^{-1} \sum_{ab} \langle a || \hat{O}_\lambda || b \rangle \langle QRPA || [c_a^+ \tilde{c}_b]_\lambda || \omega; JM \rangle . \quad (14)$$

Here the first factor  $\langle a || \hat{O}_\lambda || b \rangle$  can be calculated model independently for a given single particle basis [29]. Ground and excited states developed in the previous subsection are exploited for the second factor with the Quasi Boson Approximation (QBA). By using the phonon operator  $Q_{JM}^{+,m}$  in Eq.(8), we obtain the following expression for NC and CC

neutrino reactions. For NC reaction,

$$\begin{aligned}
& \langle QRPA || \hat{O}_\lambda || \omega; JM \rangle \\
= & \sum_{\alpha\alpha' b\beta'} [\mathcal{N}_{\alpha\alpha' b\beta'} \langle \alpha\alpha' || \hat{O}_\lambda || b\beta' \rangle [u_{pa\alpha'} v_{pb\beta'} X_{\alpha\alpha' b\beta'} + v_{pa\alpha'} u_{pb\beta'} Y_{\alpha\alpha' b\beta'}] \\
& - (-)^{j_a + j_b + J} \mathcal{N}_{b\beta' \alpha\alpha'} \langle b\beta' || \hat{O}_\lambda || \alpha\alpha' \rangle [u_{pb\beta'} v_{pa\alpha'} X_{\alpha\alpha' b\beta'} + v_{pb\beta'} u_{pa\alpha'} Y_{\alpha\alpha' b\beta'}]] + (p \rightarrow n),
\end{aligned} \tag{15}$$

where the normalization factor is given as  $\mathcal{N}_{\alpha\alpha' b\beta'}(J) = \sqrt{1 - \delta_{ab} \delta_{\alpha'\beta'} (-1)^{J+T} / (1 + \delta_{ab} \delta_{\alpha'\beta'})}$ . Without the np pairing correlation, this expression can be reduced to the following simple form

$$\begin{aligned}
& \langle QRPA || \hat{O}_\lambda || \omega; JM \rangle \\
= & \sum_{ab} [\mathcal{N}_{apbp} \langle ap || \hat{O}_\lambda || bp \rangle [u_{pa} v_{pb} X_{apbp} + v_{pa} u_{pb} Y_{apbp}] \\
& - (-)^{j_a + j_b + J} \mathcal{N}_{bpap} \langle bp || \hat{O}_\lambda || ap \rangle [u_{pb} v_{pa} X_{apbp} + v_{pb} u_{pa} Y_{apbp}]] + (p \rightarrow n),
\end{aligned} \tag{16}$$

where summations for  $\alpha'$  and  $\beta'$  are performed in Eq.(15) since quasi particle  $\alpha'$  and  $\beta'$  ( $= 1, 2$ ) include the np pairing. On the other hand, for CC reaction, they are given as

$$\begin{aligned}
& \langle QRPA || \hat{O}_\lambda || \omega; JM \rangle \\
= & \sum_{\alpha\alpha' b\beta'} [\mathcal{N}_{\alpha\alpha' b\beta'} \langle \alpha\alpha' || \hat{O}_\lambda || b\beta' \rangle [u_{pa\alpha'} v_{nb\beta'} X_{\alpha\alpha' b\beta'} + v_{pa\alpha'} u_{nb\beta'} Y_{\alpha\alpha' b\beta'}]].
\end{aligned} \tag{17}$$

This form is also easily reduced to the results by pnQRPA without pn pairing

$$\langle QRPA || \hat{O}_\lambda || \omega; JM \rangle = \sum_{apbn} [\mathcal{N}_{apbn} \langle ap || \hat{O}_\lambda || bn \rangle [u_{pa} v_{nb} X_{apbn} + v_{pa} u_{nb} Y_{apbn}]]. \tag{18}$$

As a simple application of the above form, we can calculate  $\beta^\pm$  decay, whose operator is defined as

$$\beta_{LM}^- = \hat{L}^{-1} \langle p || \hat{\beta} || n \rangle [c_p^+ \tilde{c}_n]_{LM}, \quad \beta_{LM}^+ = (\beta_{LM}^-)^+ = (-)^M \beta_{L, -M}^-, \tag{19}$$

as follows in our QRPA formalism [24],

$$\begin{aligned}
\langle 1_m^+ || \tau^+ \bar{\sigma} || 0_i^+ \rangle &= \sum_{\alpha\alpha' \beta'} [X_{(\alpha\alpha' \beta')}^m u_{\alpha\alpha' p} v_{\beta' n} + Y_{(\alpha\alpha' \beta')}^m v_{\alpha\alpha' p} u_{\beta' n}] Coef(a, b), \\
\langle 0_f^+ || \tau^+ \bar{\sigma} || 1_{m'}^+ \rangle &= \sum_{\alpha\alpha' \beta'} [\bar{X}_{(\beta\beta' \alpha')}^{m'} \bar{v}_{\alpha\alpha' p} \bar{u}_{\beta' n} + \bar{Y}_{(\beta\beta' \alpha')}^{m'} \bar{u}_{\alpha\alpha' p} \bar{v}_{\beta' n}] Coef(b, a)
\end{aligned} \tag{20}$$

with

$$Coef(a, b) = 2 \langle (l_a \frac{1}{2}) j_a || \sigma || (l_b \frac{1}{2}) j_b \rangle. \tag{21}$$



### D. Neutral and Charged Current Operators

For nuclear weak current operators, we start from a weak current on the nucleon level. The weak current operator  $W^\mu$  takes a  $V^\mu - A^\mu$  current form by the standard electro-weak theory, which has isoscalar and isovector parts for the NC interaction [24]

$$\begin{aligned} W^\mu &= V_3^\mu - A_3^\mu - 2\sin^2\theta_W J_{em}^\mu - \frac{1}{2}(V_s^\mu - A_s^\mu) \\ &= (1 - 2\sin^2\theta_W)V_3^\mu - A_3^\mu - 2\sin^2\theta_W V_0^\mu - \frac{1}{2}(V_s^\mu - A_s^\mu), \end{aligned} \quad (22)$$

with Weinberg angle  $\theta_W$ , where we used  $J_{em}^\mu = V_3^\mu + V_0^\mu$ .  $V_3^\mu (= V_{1+i2}^\mu)$  and  $A_3^\mu (= A_{1+i2}^\mu)$  are plus components of the isovector  $V_i^\mu$  and  $A_i^\mu$  by isospin rotation. Strangeness contributions, which are isoscalar parts, could be considered in  $-\frac{1}{2}(V_s^\mu - A_s^\mu)$ .

For the CC interaction, only  $V_3^\mu - A_3^\mu$  term is involved, while  $J_{em}^\mu = V_3^\mu + V_0^\mu$  is concerned with meson electro-production. Therefore the CC reaction of the  $\nu(\bar{\nu})$  scattering is nearly independent of the strangeness contents. For the elastic scattering of polarized electron on the nucleon,  $J^\mu = -2\sin^2\theta_W J_{em}^\mu - \frac{1}{2}V_s^\mu$  is exploited.

For a free nucleon, the current operator comprises the vector, the axial vector and the pseudo scalar form factor,  $F_i^V(Q^2)$ ,  $F_A(Q^2)$  and  $F_P(Q^2)$

$$W^\mu = F_1^V(Q^2)\gamma^\mu + F_2^V(Q^2)\frac{i}{2M_N}\sigma^{\mu\nu}q_\nu + F_A(Q^2)\gamma^\mu\gamma^5 + \frac{F_P(Q^2)}{2M}q^\mu\gamma^5, \quad (23)$$

where we take the scalar and the tensor form factor to be zero because of current conservation and no existence of second class current, respectively. By the conservation of the vector current (CVC) hypothesis with the inclusion of the isoscalar strange quark contributions  $F_i^s(Q^2)$ , and the vector form factors for protons and neutrons  $F_i^{V, p(n)}(Q^2)$  are expressed as [32]

$$\begin{aligned} F_i^{V, p(n)}(Q^2) &= \left(\frac{1}{2} - 2\sin^2\theta_W\right)F_i^{p(n)}(Q^2) - \frac{1}{2}F_i^{n(p)}(Q^2) - \frac{1}{2}F_i^s(Q^2) \quad \text{for NC} \\ &= (F_i^p(Q^2) - F_i^n(Q^2)) \quad \text{for CC}. \end{aligned} \quad (24)$$

The axial form factor is usually given by [33]

$$\begin{aligned} F_A^{NC}(Q^2) &= \frac{1}{2}(\mp g_A + g_A^s)/(1 + Q^2/M_A^2)^2 \quad \text{for NC} \\ F_A^{CC}(Q^2) &= -g_A/(1 + Q^2/M_A^2)^2 \quad \text{for CC}, \end{aligned} \quad (25)$$

where  $g_A$  and  $M_A$  are the axial coupling constant and the axial cut off mass, respectively.  $-(+)$  coming from the isospin dependence denotes the knocked-out proton (neutron),

respectively. Since the energy region considered here is below the quasi-elastic region, the strangeness contributions are not taken into account in this report. Since we take + sign for  $F_A(Q^2)$  in Eq.(23), the axial form factor in Eq.(25) is just negative to the form factor elsewhere, for example, in Ref.[32].

### E. Relevant Operators for weak interactions

In order to calculate weak interactions with nuclei, one resorts to the Hamiltonian,  $\mathcal{H}(\mathbf{x}) = -\frac{G_F}{\sqrt{2}} \int d\mathbf{x} \hat{W}_\mu^{weak}(\mathbf{x}) A_\mu(q\mathbf{x})$ , contracted with weak hadron (nuclear) current operator,  $\hat{W}_\mu^{weak}(\mathbf{x})$  and external weak field,  $A_\mu(q\mathbf{x}) = l_\mu \exp(-i\mathbf{q} \cdot \mathbf{x})$  with  $q = |\mathbf{q}|$  and lepton current  $l_\mu$  [2]. Here we follow the kinematics at Ref. [30]. Four momentum transfer is defined as  $q^2 (= q_\mu^2 = (k_\mu - \nu_\mu)^2) = q_0^2 - \mathbf{q}^2 = -Q^2 \leq 0$ , where  $k_\mu$  and  $\nu_\mu$  are final and initial lepton momenta. The excitation energy of a compound nucleus is given as  $\omega = -q_0 \geq 0$ .

The weak field can be expanded in terms of multipole operators by using two basic operators

$$M_J^{M_J}(q\mathbf{x}) = j_J(q\mathbf{x}) Y_J^{M_J}(\Omega_x), \quad \mathbf{M}_{JL}^{M_J}(q\mathbf{x}) = j_J(q\mathbf{x}) \mathbf{Y}_{JL1}^{M_J}(\Omega_x), \quad (26)$$

where vectorial spherical harmonic  $\mathbf{Y}_{JL1}^{M_J}(\Omega_x)$  is expressed in term of spherical harmonic  $Y_L^m(\Omega_x)$ , *i.e.*  $\mathbf{Y}_{JL1}^{M_J}(\Omega_x) = \sum_{m\lambda} \langle Lm1\lambda | (L1)JM_J \rangle Y_L^m(\Omega_x) \mathbf{e}_\lambda$ . If we make non-relativistic reduction of the one body nucleon operator using Dirac wave function, we reexpress the one-body weak transition current in terms of 4 different transition operators (Coulomb, longitudinal, electric and magnetic) as follows

$$\begin{aligned} \hat{\mathcal{M}}_{JM;TM_T}(q\mathbf{x}) &= [F_1^{(T)} M_J^{M_J}(q\mathbf{x}) - i\frac{q}{M} [F_A^{(T)} \Omega_J^{M_J}(q\mathbf{x}) + \frac{F_A - \omega F_P^{(T)}}{2} \Sigma_J^{\prime\prime M_J}(q\mathbf{x})]] I_T^{M_T} \\ \hat{\mathcal{L}}_{JM;TM_T}(q\mathbf{x}) &= [\frac{-\omega}{q} F_1^{(T)} M_J^{M_J}(q\mathbf{x}) + i(F_A^{(T)} - \frac{q^2}{2M_N} F_P^{(T)}) \Sigma_J^{\prime\prime M_J}(q\mathbf{x})] I_T^{M_T}, \\ \hat{\mathcal{T}}_{JM;TM_T}^{el}(q\mathbf{x}) &= [\frac{q}{M} [F_1^{(T)} \Delta_J^{\prime M_J}(q\mathbf{x}) + \frac{1}{2} \mu^{(T)} \Sigma_J^{M_J}(q\mathbf{x})] + iF_A^{(T)} \Sigma_J^{\prime M_J}(q\mathbf{x})] I_T^{M_T}, \\ \hat{\mathcal{T}}_{JM;TM_T}^{mag}(q\mathbf{x}) &= -i\frac{q}{M} [[F_1^{(T)} \Delta_J^{M_J}(q\mathbf{x}) - \frac{1}{2} \mu^{(T)} \Sigma_J^{\prime M_J}(q\mathbf{x})] + F_A^{(T)} \Sigma_J^{M_J}(q\mathbf{x})] I_T^{M_T}, \end{aligned} \quad (27)$$

where the superscript  $T(= 0, 1)$  means isoscalar and isovector. The 8 relevant single particle operators ( $M_J^{M_J}, \Omega_J^{M_J}, \Omega_J^{\prime M_J}, \Sigma_J^{M_J}, \Delta_J^{M_J}, \Sigma_J^{\prime M_J}, \Sigma_J^{\prime\prime M_J}, \Delta_J^{\prime M_J}$ ) are given as follows,

whose detailed derivation was done at Ref. [2, 29],

$$\begin{aligned}
M_J^M & , & (28) \\
\Delta_J^{M_J} & = \mathbf{M}_{JJ}^{M_J}(q\mathbf{x}) \cdot \frac{1}{q} \nabla , \\
\Delta_J^{\prime M_J} & = [J]^{-1} [-J^{\frac{1}{2}} \mathbf{M}_{JJ+1}^{M_J}(q\mathbf{x}) + (J+1)^{1/2} \mathbf{M}_{JJ-1}^{M_J}(q\mathbf{x})] \cdot \frac{1}{q} \nabla \\
\Sigma_J^{M_J} & = \mathbf{M}_{JJ}^{M_J}(q\mathbf{x}) \cdot \sigma , \quad \Sigma_J^{\prime M_J} = [J]^{-1} [-J^{\frac{1}{2}} \mathbf{M}_{JJ+1}^{M_J}(q\mathbf{x}) + (J+1)^{1/2} \mathbf{M}_{JJ-1}^{M_J}(q\mathbf{x})] \cdot \sigma \\
\Sigma_J^{\prime\prime M_J} & = [J]^{-1} [(J+1)^{\frac{1}{2}} \mathbf{M}_{JJ+1}^{M_J}(q\mathbf{x}) + J^{1/2} \mathbf{M}_{JJ-1}^{M_J}(q\mathbf{x})] \cdot \sigma \\
\Omega_J^{M_J}(q\mathbf{x}) & = M_J^{M_J}(q\mathbf{x}) \sigma \cdot \frac{1}{q} \nabla , \quad \Omega_J^{\prime M_J}(q\mathbf{x}) = \Omega_J^{M_J}(q\mathbf{x}) + 1/2 \Sigma_J^{\prime\prime M_J}(q\mathbf{x}) .
\end{aligned}$$

In actual calculation, the last operator is not used because it can be combined by other operators [10]. Single nucleon form factors in Eq.(27) are denoted as  $F_X^{(T)}(Q^2)$  with  $T = 0, 1$  and  $X = 1, 2, A, P$  standing for Dirac ( $X=1$ ), Pauli ( $X=2$ ), axial, and pseudoscalar form factors, respectively. Detailed form factors are referred from Ref. [2, 29]. The induced pseudoscalar form factor is usually parameterized by the Goldberger-Treiman relation

$$F_P(Q^2) = \frac{2M_N}{Q^2 + m_\pi^2} F_A(Q^2), \quad (29)$$

where  $m_\pi$  is the pion mass. The contribution of the pseudoscalar form factor vanishes for the NC reaction because of the negligible final lepton mass participating in this reaction. But it can contribute to the CC reaction, in particular, for  $\nu_\mu - A$  reaction.

## F. Cross Sections

Based on the initial and final nuclear states, cross section for  $\nu(\bar{\nu}) - A$  scattering through the relevant transition operator in Eq.(27) is given as [30]

$$\begin{aligned}
\left(\frac{d\sigma_\nu}{d\Omega}\right)_{(\nu/\bar{\nu})} & = \frac{G_F^2 \epsilon k}{\pi (2J_i + 1)} \left[ \sum_{J=0} (1 + \vec{\nu} \cdot \vec{\beta}) | \langle J_f | \hat{\mathcal{M}}_J | J_i \rangle |^2 \right. & (30) \\
& + (1 - \vec{\nu} \cdot \vec{\beta} + 2(\hat{\nu} \cdot \hat{q})(\hat{q} \cdot \vec{\beta})) | \langle J_f | \hat{\mathcal{L}}_J | J_i \rangle |^2 - \hat{q} \cdot (\hat{\nu} + \vec{\beta}) 2Re \langle J_f | \hat{\mathcal{L}}_J | J_i \rangle \langle J_f | \hat{\mathcal{M}}_J | J_i \rangle^* \\
& + \sum_{J=1} (1 - (\hat{\nu} \cdot \hat{q})(\hat{q} \cdot \vec{\beta})) (| \langle J_f | \hat{\mathcal{T}}_J^{el} | J_i \rangle |^2 + | \langle J_f | \hat{\mathcal{T}}_J^{mag} | J_i \rangle |^2) \\
& \left. \pm \sum_{J=1} \hat{q} \cdot (\hat{\nu} - \vec{\beta}) 2Re [ \langle J_f | \hat{\mathcal{T}}_J^{mag} | J_i \rangle \langle J_f | \hat{\mathcal{T}}_J^{el} | J_i \rangle^* ] \right] ,
\end{aligned}$$

where  $(\pm)$  means the case of  $\nu(\bar{\nu})$ , respectively.  $\vec{\nu}$  and  $\vec{k}$  are incident and final lepton 3-momenta, and  $\vec{q} = \vec{k} - \vec{\nu}$ ,  $\vec{\beta} = \vec{k}/\epsilon$  with the final lepton's energy  $\epsilon$ . Of course, the

extremely relativistic limit (ERL) may yield more simple formula, but we use the general expression for the  $\nu_\mu - A$  reaction. For CC reaction we multiplied Cabbibo angle  $\cos^2\theta_c$  and include the Coulomb distortion of the outgoing leptons due to the residual nucleus [3, 10].

Since the Fermi function,  $F(Z \pm 1, \epsilon_f)$ , is deduced for the outgoing electron in the  $\beta$  decay [34], which usually assumed s-wave electron, one needs more deliberate approach for  $\nu - A$  reactions, in which outgoing lepton energy is higher rather than that of the  $\beta$  decay. To exactly describe the Coulomb distortion, one needs to solve the Dirac equation of the outgoing lepton under the Coulomb potential due to the residual interactions with daughter nucleus [35, 36]. But, since the exact solution needs a time consuming computation, one usually exploits the averaged momentum of the outgoing particles. Typical method is the effective momentum approach (EMA), which is able to reproduce exact calculations more or less [10, 37, 38]. Here we use both approaches, the Fermi function and the EMA approach. By following the prescriptions on Ref.[10, 21], below the energy on which both approaches predict same values, the Fermi function is used, while the EMA is adopted above the energy region.

### III. RESULTS

#### A. $\nu(\bar{\nu}) - {}^{12}\text{C}$ reaction

In Fig.1, we show the cross sections of  ${}^{12}\text{C}(\nu_e, e^-){}^{12}\text{N}^*$  reaction for  $J^\pi = 0^\pm \sim 4^\pm$  states with dominant transitions ( $0^+, 1^\pm$  and  $2^-$  states' contributions) and total sum of all states. Other states' contributions not indicated here are within only a few percentage. Experimental LSND data for the exclusive  ${}^{12}\text{C}(\nu_e, e^-){}^{12}\text{N}_{g.s.(1^+)}$  reaction are taken from Ref. [11]. Our results for the Gamow Teller  $1^+$  state clearly reproduce the data. Other  $J^\pi$  states' contributions including spin dipole resonances turned out to become also important for understanding the  $\nu - {}^{12}\text{C}$  reaction via CC [3, 10], in specific, beyond 45 MeV energy region.

Results for the NC reaction,  ${}^{12}\text{C}(\nu, \nu'){}^{12}\text{C}^*$ , are shown in Fig.2. Remarkable point is that the GT transition dominates overwhelmingly the cross section by NC. Below the 55 MeV region, other transitions contribute within only a few %. This is contrast to those for CC reactions. Energy folded (or flux averaged) cross sections by Eq.(2) for the exclusive

and the inclusive reaction via CC and NC reactions are tabulated in table 1 with other theoretical results and experimental data.

In order to pin down the ambiguities from the nuclear structure, results for  $\beta$  decay are also shown in table I. Here we used  $g_A = 1.23$  from Ref. [2], which reproduces half lives of  $\beta^-$  and  $\beta^+(EC)$  decays, as shown in table 1. For pairing interactions,  $g_{nn} = 1.6149$ ,  $g_{pp} = 1.4988$  and  $g_{np} = 2.0698$  are adjusted to fit the empirical pairing gaps  $\Delta_{nn} = 4.548$ ,  $\Delta_{pp} = 4.430$  and  $\delta_{np} = 2.489$  MeV, respectively [24].

Our QRPA results reproduce most of the experimental data and show reasonable consistency with other theoretical model calculations. But the  $\langle \sigma \rangle$  for the exclusive reaction,  $^{12}\text{C}(\nu_e, e^-)^{12}\text{N}_{g.s.}$ , in table 1 overestimates the data about 10 % maximally. It might be understood from the following discussion about the Coulomb distortion.

Main contributions to the folded cross section of the exclusive reaction come from the energy region  $E_{\nu_e} \leq 52$  MeV because of the Michel spectrum, Eq.(3). We divide the energy region into two regions for the Coulomb correction. In the energy region below 45 MeV, we take the Fermi function. But the Gamow Teller  $1^+$  state transition,  $^{12}\text{C}(\nu_e, e^-)^{12}\text{N}_{g.s.}$ , overestimates the experimental data about 7 ~ 8 % as shown in Fig.1. This is the reason for the overestimation of the folded cross section.

Here we discuss the Coulomb distortion effect. In Fig.3, we show three different results ; Fermi function correction, effective momentum approach (EMA) [10] and no Coulomb correction. The Fermi function correction turns out to be larger than the EMA correction in the energy region above 60 MeV, which confirmed discussions in Refs. [9, 10]. But, in the energy region  $45 \leq E_{\nu} \leq 60$  MeV, results by both approaches are nearly indiscernible and well reproduce the experimental data. However, below 45 MeV, the Fermi function and the EMA overestimate the cross sections about 7 ~ 8 % and 10 ~ 12 %, respectively, while the case of no Coulomb correction seems to match with the data. Therefore, for more exact result within 1 or 2 % for the flux averaged cross section for the  $^{12}\text{C}(\nu_e, e^-)^{12}\text{N}_{g.s.}$ , more careful treatment of Coulomb corrections in the low energy region would be necessary.

Our QRPA includes not only proton-proton and neutron-neutron pairing but also neutron-proton (np) pairing, but the contribution by the np pairing turns out to be only within 1 ~ 2 % for the relevant weak interaction in  $^{12}\text{C}$ , such as  $\beta^\pm$  decay and the  $\nu-^{12}\text{C}$  reaction. Since the energy gap between neutron and proton space is relatively large in light nuclei, the neutron-proton pairing is expected to be small. But in the medium-

heavy or heavy nuclei, the effect could be larger as shown in the results for  $\nu$ - $^{56}\text{Ni}$ ( $^{56}\text{Fe}$ ) reactions.

### B. $\nu(\bar{\nu})$ - $^{56}\text{Ni}$ and $\nu(\bar{\nu})$ - $^{56}\text{Fe}$ reaction

Here we calculate reactions of  $^{56}\text{Ni}(\nu_e, \nu'_e)^{56}\text{Ni}^*$ ,  $^{56}\text{Ni}(\bar{\nu}_e, \bar{\nu}'_e)^{56}\text{Ni}^*$  via NC, and  $^{56}\text{Fe}(\nu_e, e^-)^{56}\text{Co}^*$  via CC. Results for  $\nu(\bar{\nu})$ - $^{56}\text{Ni}$  by NC are shown in Fig.4 and 5. Remarkable difference between  $\nu_e$ - and  $\bar{\nu}_e$  - $^{56}\text{Ni}$  is the magnitude of cross sections, in which cross sections by  $\nu_e$  reaction are about 40 % larger than those by  $\bar{\nu}_e$  reaction. But the cross section is dominated by the GT transition. Contributions by higher multipole transitions are shown to be within only a few %, similarly to the case of  $^{12}\text{C}(\nu_e, \nu'_e)^{12}\text{C}^*$ . Higher multipole contributions to the NC reaction turns out to be much smaller than those to the CC reaction. It is also confirmed in  $^{56}\text{Fe}(\nu_e, e^-)^{56}\text{Co}^*$  reaction as shown in Fig.6.

Fermi function for the Coulomb corrections is used on the energy region below 45 MeV and the EMA is taken beyond 45 MeV. For pairing interactions,  $g_{nn} = 1.3134(1.0244)$ ,  $g_{pp} = 1.1558(1.0340)$  and  $g_{np} = 1.2785(1.3057)$  are adjusted to the empirical pairing gaps  $\Delta_{nn} = 2.148(1.425)$ ,  $\Delta_{pp} = 2.078(1.572)$  and  $\delta_{np} = 1.102(0.336)$  MeV for  $^{56}\text{Ni}$  ( $^{56}\text{Fe}$ ) nucleus, respectively [24].

Since we have an experimental data for  $^{56}\text{Fe}(\nu_e, e^-)^{56}\text{Co}^*$  by the DAR neutrino given as energy weighted cross section, which is the only experimental  $\nu - A$  reaction data beyond  $^{12}\text{C}$ , we compared our results to the experimental data. If the np pairing is switched off, we obtain  $\langle \sigma \rangle = 141.8 \times 10^{-42} \text{cm}^2$ . But the np pairing enhanced it to  $173.5 \times 10^{-42} \text{cm}^2$  which is located within the experimental data  $256 \pm 108 \pm 43 \times 10^{-42} \text{cm}^2$ . As discussed in Ref. [10], previous QRPA calculations without np pairing could not reproduce the experimental data.

In Fig.7, we show GT strength feasible from the (p,n) or (n,p) reaction on  $^{56}\text{Fe}$  or  $^{56}\text{Ni}$  target. They are calculated as

$$B(GT_{\pm}) = \frac{1}{2J_i + 1} | \langle f | | \sum_k \sigma_k \tau_{k\mp} | | i \rangle |^2 . \quad (31)$$

Results in Fig.7 did not use the quenching factor. Our results for total GT strength with the quenching factor  $f_q = 0.74$  are 11.38 and 4.41 for  $B(GT_{\mp})$ . They are consistent with those of experimental data,  $9.9 \pm 2.4$  [39] and  $2.8 \pm 0.3$  [40], respectively. As shown in

Fig.7, contributions from the higher excited states lead to a bit larger value for  $B(GT_+)$  than the data. Similarly to the results by the shell model [6], which is a hybrid model *i.e.* shell model for GT and IAS transition and QRPA model for high multipole transitions, our results reproduced the experimental data by using the same quenching factor as the shell model. We expect that more fruitful data for the relevant weak transitions, which enables to constraint the ambiguities from the nuclear structure.

For higher multipoles we did not use the quenching factor by following the discussions at Ref. [6]. But larger contributions compared to those by Ref. [6] are obtained for the higher multipole transitions. In Ref. [6], 80 % of the data is explained by the GT and IAS transition. Therefore our results explain systematically the  $\nu$ - $^{56}\text{Fe}$  and  $\nu$ - $^{56}\text{Ni}$  reaction as well as the GT strength in the single  $\beta$  decay in a systematically organized QRPA model. For the supernovae application, we show the cross sections averaged by the SN neutrino spectrum in Eq.(1) in Fig. 8. Cross section via CC are much larger, about 3 times, than those by NC, irrespective of nucleus species. Application to the  $\nu$  process for other relevant nuclei are in progress.

#### IV. SUMMARY AND CONCLUSION

We applied the QRPA to the  $\nu - A$  reaction by including multipole transitions up to  $J^\pi = 4^\pm$  with explicit momentum dependence and evaluated the  $\nu$ -reaction to  $^{12}\text{C}$ ,  $^{56}\text{Ni}$  and  $^{56}\text{Fe}$  target. Our results for the  $\nu(\bar{\nu}) - A$  reaction show quite consistent results with available experimental data and other theoretical calculations.

Remarkable points from our results are summarized as follows. Firstly, not only GT, IAS and spin dipole transitions but also other multipole transitions could play roles for  $\nu - A$  reaction via CC below the quasi elastic peak. But NC reaction is dominated by the GT transition.

Secondly, np pairing as well as nn and pp pairing correlations act as important ingredients for describing the BCS ground state, and contribute to some extent to the cross section of the  $\nu - A$  reaction. In particular, it affects the results for medium heavy nuclei such as  $^{56}\text{Ni}$  and  $^{56}\text{Fe}$ , which was already expected from our previous results for  $2\nu 2\beta$  and  $0\nu 2\beta$  decays.

Finally, for more exact evaluation within a few % for the flux averaged cross section

of the future would-be experimental data, more deliberately chosen Coulomb correction would be necessary. In particular, experimental data via NC would be desirable to pin down the ambiguities on the Coulomb corrections.

The QRPA is a very efficient method to consider multi-particle and multi-hole interactions and their configuration mixing, which successfully described nuclear reactions sensitive on the nuclear structure, such as  $2\nu 2\beta$  and  $0\nu 2\beta$  decays. Therefore the ambiguities feasible due to the nuclear structure can be pinned down by reproducing the data related to the  $\beta$  and  $\beta\beta$  decay. The extension of our QRPA calculation for  $\nu - A$  reaction to explicitly include the deformation [41], which turns out to be so important for the exotic nuclei frequently appeared, is under progress. It enables us to perform various nuclear weak reactions for stable and unstable nuclei.

This work was supported by the Korea Research Foundation Grant funded by the Korean Government(MOEHRD, Basic Research Promotion Fund)(KRF-2006-331-C00078) and one of author, Cheoun, was supported by the Soongsil University Research Fund.

- 
- [1] W. L. Freedman and M. S. Turner, Rev. of Modern Phys. **75**, 1433 (2003).
  - [2] J. S. O'Connell, T. W. Donnelly, and J. D. Walecka, Phys. Rev. C **6**, 719 (1972).
  - [3] T. Suzuki, S. Chiba, T. Yoshida, T. Kajino, T. Otsuka, Phys. Rev. C **74**, 034307 (2006).
  - [4] S. E. Woosley, D. H. Hartmann, R. D. Hoffmann, and W. C. Haxton, Astrophys. J. **356**, 272 (1990).
  - [5] T. Yoshida, T. Suzuki, S. Chiba, T. Kajino, H. Yokomukura, K. Kimura, A. Takamura, H. Hartmann, Astro. Phys. J. **686**, 448 (2008).
  - [6] T. Suzuki, M. Honma, K. Higashiyama, T. Yoshida, T. Kajino, T. Otsuka, H. Umeda, and K. Nomoto, Phys. Rev. C **79**, 061603 (2009).
  - [7] A. Heger, E. Kolbe, W.C. Haxton, K. Langanke, G. Martinez-Pinedo and S.E. Woosley, Phys. Lett. B **606**, 258 (2005).
  - [8] Shinya Wanaajo, Astrophys. J. **647**, 1323 (2006).
  - [9] E. Kolbe, K. Langanke, G. Martinez-Pinedo and P. Vogel, J. Phys. G **29**, 2569 (2003).



- [10] N. Paar, D. Vretenar, T. Marketin, and P. Ring, Phys. Rev. C **77**, 024608 (2008).
- [11] C. Athanasopoulos *et al.*, (LSND Collaboration), Phys. Rev. C **55**, 2078 (1997).
- [12] L. B. Auerbach *et al.* (LSND Collaboration), Phys. Rev. C **64**, 065501 (2001).
- [13] B. E. Bodmann *et al.*, (KARMEN Collaboration), Phys. Lett. **B 332**, 251 (1994).
- [14] R. Maschuw, Prog. Part. Nucl. Phys. **40**, 183 (1998).
- [15] B. A. Armbruster *et al.* (KARMEN Collaboration), Phys. Lett. **B 423**, 15 (1998).
- [16] P. Zucchelli, Phys. Lett. B **532**, 166 (2002).
- [17] Cristina Volpe, J. Phys. G **34**, R1 (2007).
- [18] Joe Sato, Phys. Rev. Lett. **95**, 131804 (2005).
- [19] Jose Bernabeu, Jordi Burguet-Castell, Catalina Espinoza, and Mats Lindroos, J. Hep. **12** 014 (2005).
- [20] W. Hauser and H. Feshbach, Phys. Rev. **87**, 366 (1952).
- [21] C. Volpe, N. Auerbach, G. Colo, T. Suzuki, and N. Van Giai, Phys. Rev. C **62**, 015501 (2000).
- [22] E. Kolbe, K. Langanke, F.-K.Thielemann, and P. Vogel, Phys. Rev. C **52**, 3437 (1995).
- [23] E. Kolbe, Nucl. Phys. **A719**, 135c (2003).
- [24] M. K. Cheoun, A. Bobyk, Amand Faessler, F. Simcovic and G. Teneva, Nucl. Phys. **A561**, 74 (1993) ; Nucl. Phys. **A564**, 329 (1993); M. K. Cheoun, G. Teneva and Amand Faessler, Prog. Part. Nuc. Phys. **32**, 315 (1994) ; M. K. Cheoun, G. Teneva and Amand Faessler, Nucl. Phys. **A587**, 301 (1995).
- [25] N. Jachowicz, K. Heyde, J. Ryckebusch, and S. Rombouts, Phys. Rev. C **65**, 025501 (2002).
- [26] Antonio Bortrungo, Giampaolo Co', Nucl. Phys. **A761**, 200 (2005).
- [27] M. Baranger, Phys. Rev.**130**, 1244 (1963).
- [28] K. Holinde, Phys. Rep. **68**, 121 (1981).
- [29] T. W. Donnelly and W. C. Haxton, ATOMIC DATA AND NUCLEAR DATA **23**, 103 (1979).
- [30] J. D. Walecka, in *Muon Physics*, edited by V. H. Huges and C. S. Wu (Academic, New York, 1975), Vol II.
- [31] Myung-Ki Cheoun and K. S. Kim, J. Phys. **G 35** 065107 (2008).

- [32] Andrea Meucci, Carlotta Giusti, and Franco Davide Pacati, Nucl. Phys. **A739**, 277 (2004); Nucl. Phys. **A744**, 307 (2004); Nucl. Phys. **A773**, 250 (2006).
- [33] M. J. Musolf and T. W. Donnelly, Nucl. Phys. **A546**, 509 (1992).
- [34] D. H. Wilkinson and B. E. F. Macefield, Nucl. Phys. **A 232**, 58 (1974).
- [35] K. S. Kim, L. E. Wright, Yanhe Jin, and D. W. Kosik, Phys. Rev. **C 54**, 2515 (1996).
- [36] K. S. Kim, L. E. Wright, and D. A. Resler, Phys. Rev. **C 64**, 044607 (2001).
- [37] A. Bortrungo and G. Co', Eur. Phys. J. **A24S1**, 109, (2005).
- [38] Giampaolo Co', Acta Physica Polonica B **37**, 2235, (2006).
- [39] J. Rapaport *et. al*, Nucl. Phys. **A 410**, 371 (1983).
- [40] E. Caurier, K. Langanke, G. Martinez-Pinedo, and F. Nowacki, Nucl. Phys. **A 653**, 439 (1999).
- [41] F. Simkovic, L. Pacearescu, and A. Faessler, Phys. Rev. **C68**, 054319 (2003); Nucl. Phys. **A733**, 321 (2004).

Table. I: Comparison of calculated and measured flux averaged cross sections for the  $\nu-^{12}\text{C}$  reaction in units of  $10^{-42}\text{cm}^2$ , and half life time of neighboring nuclei. The cross sections are folded by the corresponding DAR neutrino spectra, where the Michel spectrum is used for  $\nu_e$  and  $\nu_\mu$  energy is fixed at 29.8 MeV. "K" and "L" mean Karmen and LSND groups results, respectively. Shell Model(SM) and Continuum RPA(CRPA) results are cited from Ref.[3] and Ref.[9], respectively. (9.834\*) is a result with no Coulomb correction.

	$^{12}\text{C}(\nu_e, e^-)^{12}\text{N}_{g.s.}$	$^{12}\text{C}(\nu_e, e^-)^{12}\text{N}^*$	$\beta^{(-)} : (^{12}\text{B}(1^+) \rightarrow ^{12}\text{C})$
Exp.	$8.9 \pm 0.3 \pm 0.9$ [12]"L"	$4.3 \pm 0.4 \pm 0.6$ [12]"L"	23.6 ms
	$9.1 \pm 0.5 \pm 0.8$ [13]"K"	$5.1 \pm 0.6 \pm 0.5$ [14]"K"	
Ours	11.53 (9.834*)	6.1	21.33 ms
SM	9.06 ~ 8.48	5.22 ~ 4.87	
CRPA	8.9	5.4	
	$^{12}\text{C}[(\nu_e, \nu'_e) + (\bar{\nu}_\mu, \bar{\nu}'_\mu)]^{12}\text{N}_{g.s.}$	$^{12}\text{C}[(\nu_\mu, \nu'_\mu)]^{12}\text{C}^*$	$\beta^{(+)}(EC) : (^{12}\text{N}(1^+) \rightarrow ^{12}\text{C})$
Exp.	$10.4 \pm 1.0 \pm 0.9$ [13]"K"	$3.2 \pm 0.5 \pm 0.4$ [15]"K"	11.0 ms
Ours	9.92	3.60	10.34 ms
SM	9.76 ~ 8.27	2.68 ~ 2.26	
CRPA	10.5		

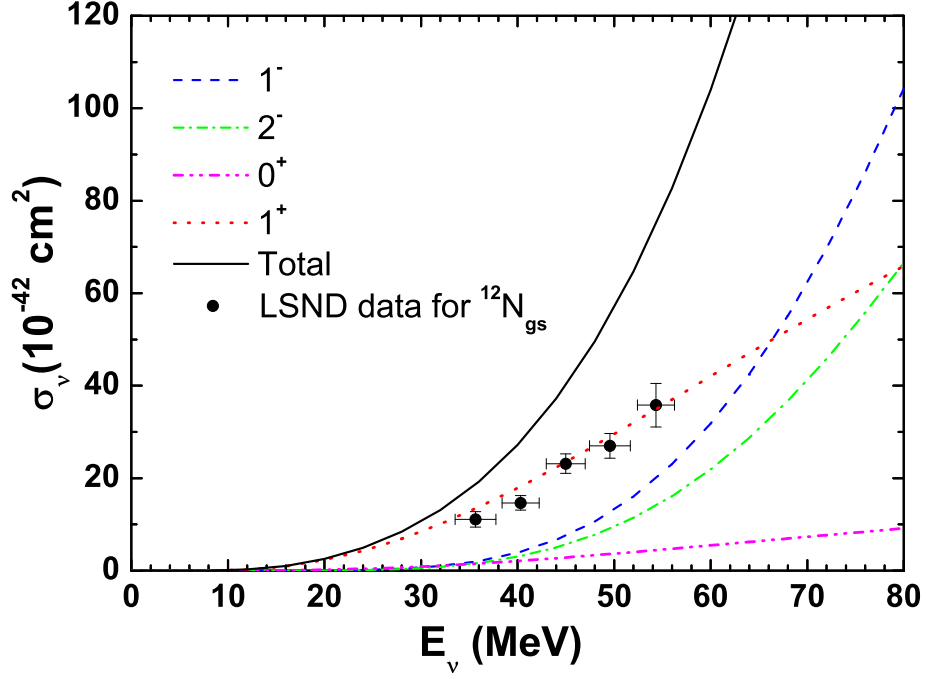


Fig. 1: (Color online) Cross sections of the  $^{12}\text{C}(\nu_e, e^-)^{12}\text{N}^*$  reaction for  $J_\pi = 0^\pm \sim 4^\pm$  states. Main multipole states ( $0^+$ ,  $1^\pm$  and  $2^-$ ) contributions and total sum are presented. Cross section via  $J^\pi = 1^+$  state is compared to the LSND experimental data,  $^{12}\text{C}(\nu_e, e^-)^{12}\text{N}_{g.s.(1^+)}$  [11].

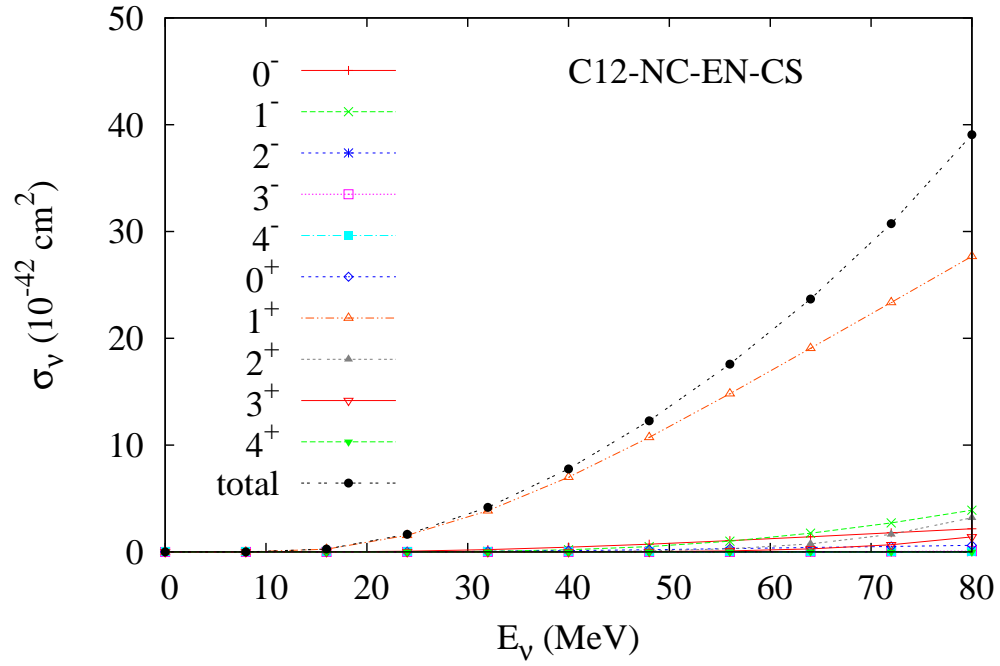


Fig. 2: (Color online) Cross sections of the  $^{12}\text{C}(\nu_e, \nu'_e)^{12}\text{C}^*$  reaction for  $J_\pi = 0^\pm \sim 4^\pm$  states. Each multipole state contribution and total sum are presented.

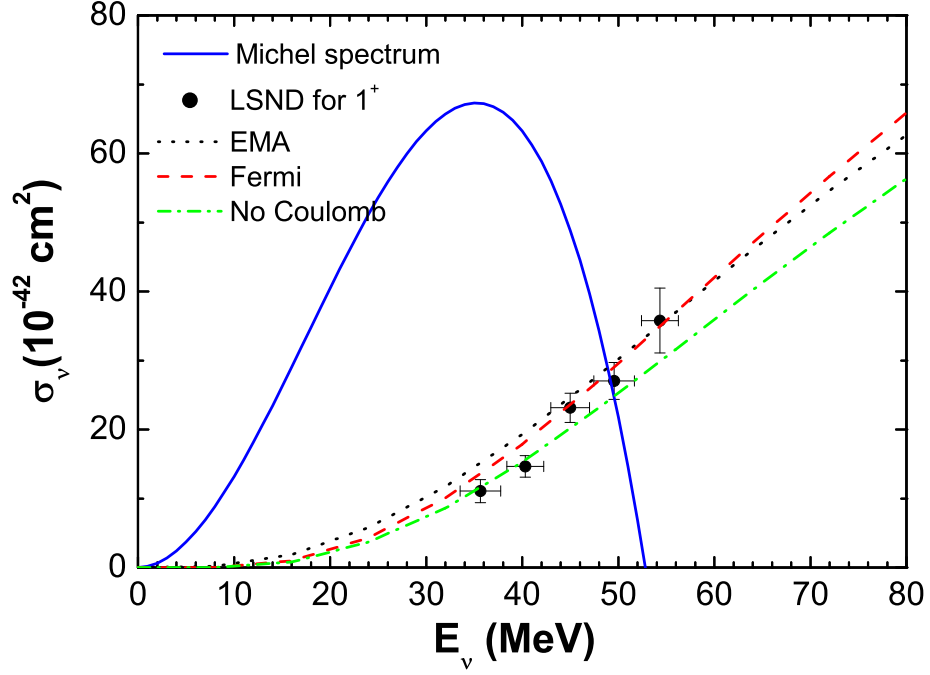


Fig. 3: (Color online) Comparison of two different Coulomb corrections and no Coulomb correction for the  $^{12}\text{C}(\nu_e, e^-)^{12}\text{N}_{g.s.(1^+)}$  reaction. Arbitrary normalized Michel spectrum for DAR neutrino is also presented to indicate the contribution by the incident neutrino energy bin to the flux averaged cross sections. Data point for the  $J^\pi = 1^+$  state is the same as Fig.1 *i.e.* the LSND data for  $^{12}\text{C}(\nu_e, e^-)^{12}\text{N}_{g.s.(1^+)}$  [11].

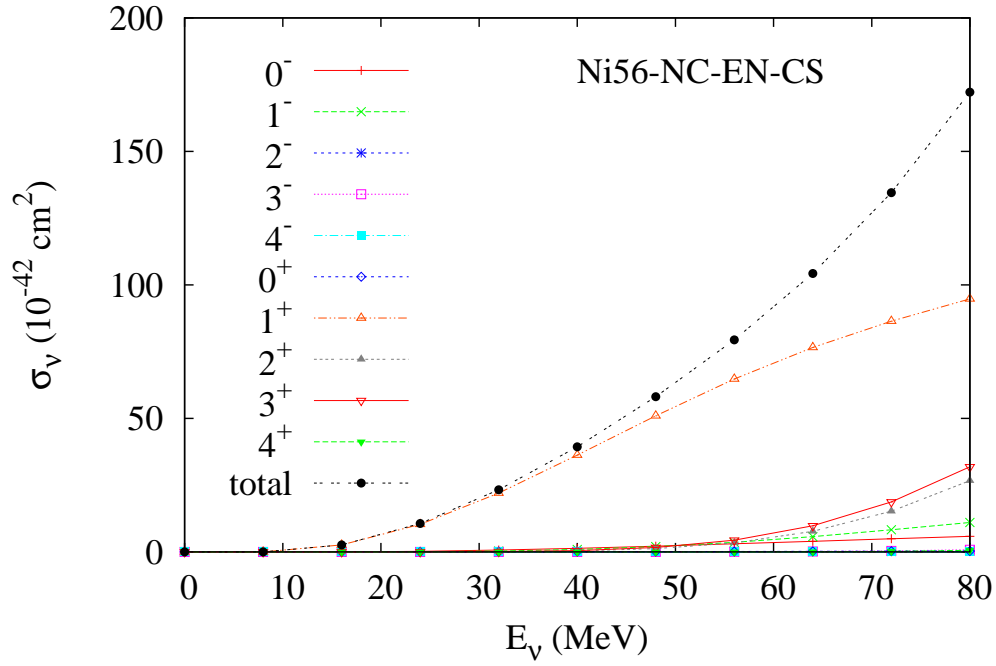


Fig. 4: (Color online) Cross sections of the  $^{56}\text{Ni}(\nu_e, \nu'_e)^{56}\text{Ni}^*$  reaction for  $J_\pi = 0^\pm \sim 4^\pm$  states. Each multipole state contribution and total sum are presented.

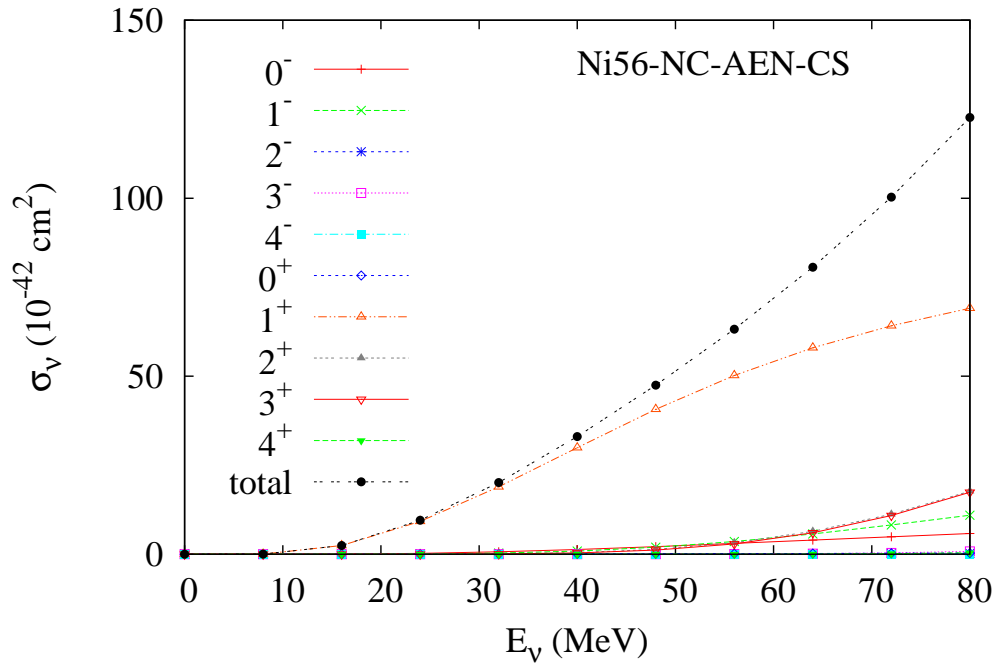


Fig. 5: (Color online) Cross sections of the  $^{56}\text{Ni}(\bar{\nu}_e, \bar{\nu}'_e)^{56}\text{Ni}^*$  reaction for  $J_\pi = 0^\pm \sim 4^\pm$  states. Each multipole state contribution and total sum are presented.

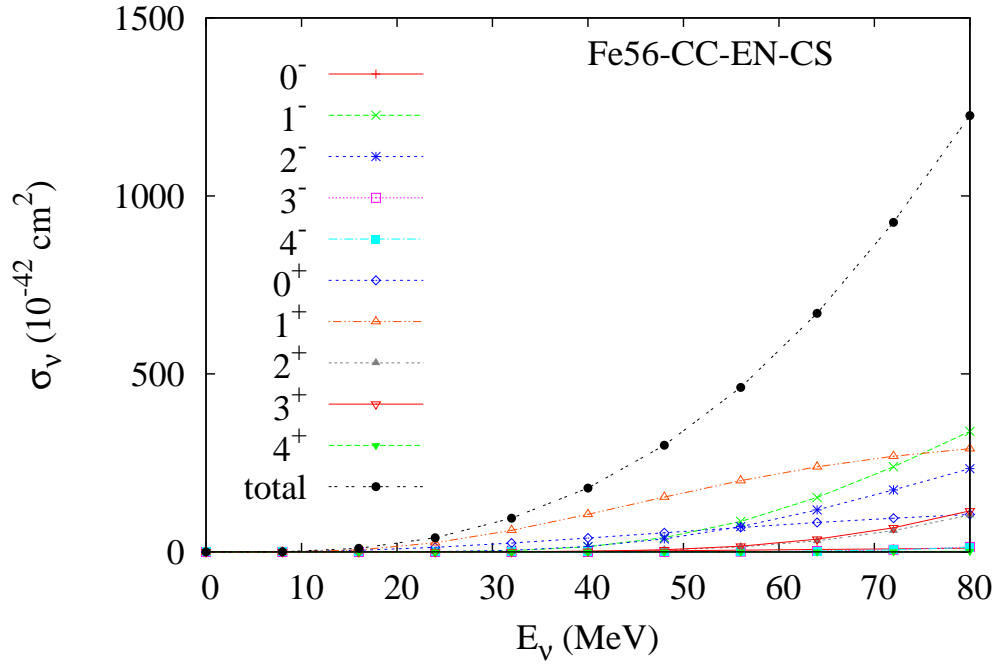


Fig. 6: (Color online) Cross sections of the  $^{56}\text{Fe}(\nu_e, e^-)^{56}\text{Co}^*$  reaction for  $J_\pi = 0^\pm \sim 4^\pm$  states. Each multipole state contribution and total sum are presented.

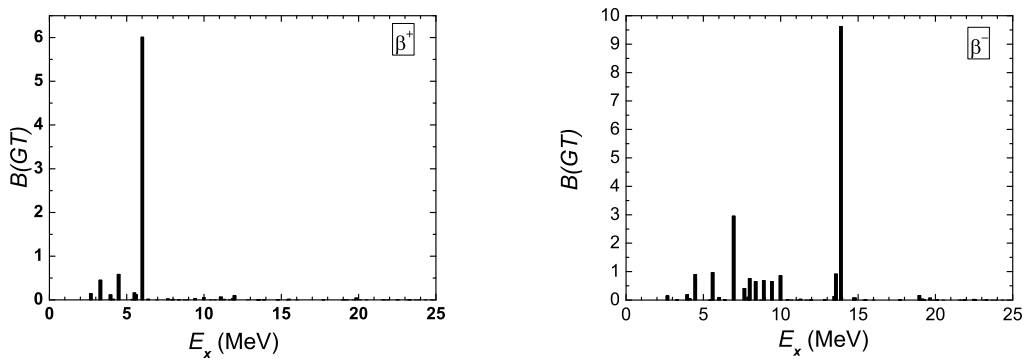


Fig. 7: (Color online) Gamow-Teller strength  $B(GT_\pm)$  for  $^{56}\text{Fe}$



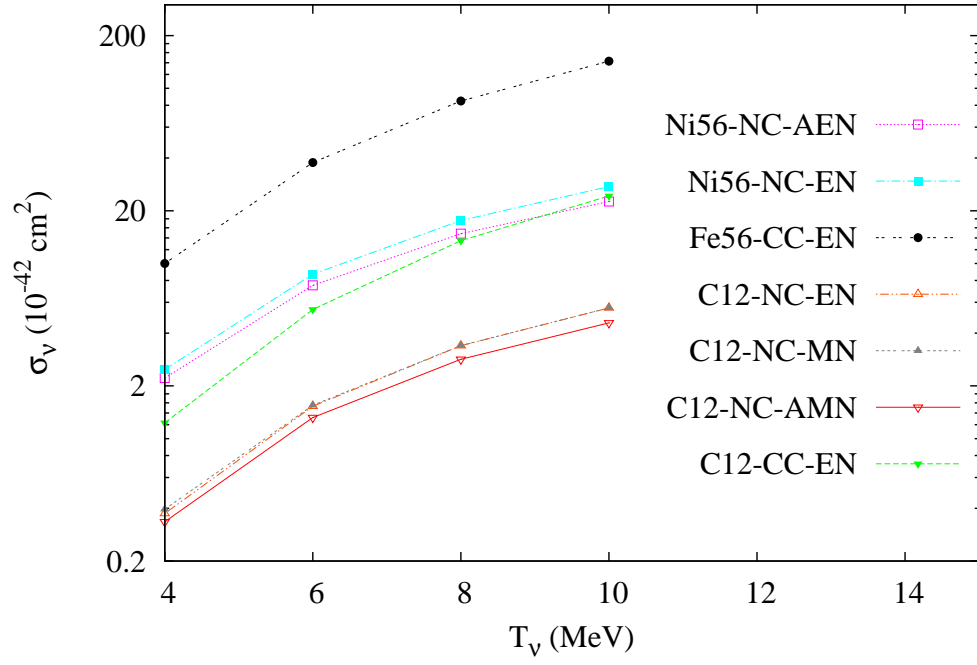


Fig. 8: (Color online) Temperature dependence of the energy weighted cross section, Eq. [2] for  $\nu$ - $^{12}\text{C}$ ,  $^{56}\text{Ni}$  and  $^{56}\text{Fe}$  reactions, where neutrino spectrum for the SN, Eq.(1), is exploited.